The recent trend of increasing precipitation in Sahel and the associated inter-hemispheric dipole of global SST

Masaki Munemoto[1] and Yoshihiro Tachibana[1,2]
509M236@m.mie-u.ac.jp tachi@bio.mie-u.ac.jp

1 : Climate and Ecosystem Dynamics Division, Mie University, Tsu, Japan

2 : Research Institute for Global Change, JAMSTEC, Yokosuka, Japan

Short Title : Increasing rainfall in Sahel and the associated global SST variation

Key Words : Sahel; precipitation; trend shift; global SST

21 November, 2010, revised

Corresponding Author :

Yoshihiro Tachibana

tachi@bio.mie-u.ac.jp

Climate and Ecosystem Dynamics Division, Mie University, Tsu, Japan

1577 Kurimamachiya-cho, Tsu City, Mie Prefecture, Japan (514-8507)

+81-59-231-9626

Abstract

Although the Sahel precipitation decreased during the 1970s, it has increased since the mid-1980s. This trend shift also occurred throughout the world with weaker signatures than in Sahel. The trend shift of precipitation over north Eurasia and Sahel regions was overall in phase, whereas those over the South America were out of phase with Sahel. The Sahel trend shift was remarkably similar to the trend shift of the difference in SSTs between Northern Hemisphere (NH) and Southern Hemisphere (SH); that is, until the 1980s the NH SST had decreased relative to the SH SST, whereas after the 1980s this trend reversed. Concurrent with this shift were trend shifts in the NH-SH contrast in atmospheric temperature and humidity and in inter-hemispheric meridional winds around Sahel. It appears that the NH-SH SST contrast determines the long-term variation of precipitation over Sahel through the shift of inter-hemispheric atmospheric circulations.

1. Introduction

The Sahel region, located along the southern fringe of the great Sahara desert, experiences a hot, desert climate for most of the year and a tropical, rainy climate for the rest. Land degradation in arid lands is now recognized as one of the most important environmental problems of the 21st century, and Sahel is often mentioned as the most seriously affected region (Thiaw and Mo, 2005). This region underwent an unprecedented severe drought associated with a decrease of precipitation in the 1970s and 1980s (e.g. Giannini et al., 2003, Hoerling et al., 2006, Nicholson and Wbster, 2007, Omotosho, 2008).

However, since the 1990s the precipitation in West Africa, including Sahel, seems to have been gradually increasing (e.g. Fall et al., 2006, Folts and McPhaden, 2008, Hagos and Cook, 2008, Omotosho 2008). Hoerling et al. (2006) also pointed out that Sahel might experience a recovery in rainfall from a low point in the 1980s to values after 2000 that consistently exceed the 1950-1999 climatology. These observations imply that some kinds of regional or global climate shifts induce the precipitation changes over Sahel. Nevertheless, as yet there is no clear explanation for the relationship between the trend shift of the Sahel precipitation in the 1980s and global climate changes.

Only a few previous studies have explained the recent increasing precipitation in terms of climate and SST variability (e.g. Hoerling et al., 2006, Folts and McPhaden, 2008, Hagos and Cook, 2008). On the basis of the results of a model simulation, Hagos and Cook (2008) emphasized that the partial recovery of precipitation during the 1990s was related mainly to the warming of the northern tropical Atlantic Ocean and the associated cyclonic circulation, which supplies Sahel with moisture. Hoerling et al. (2006) emphasized that drying over Sahel during the boreal summer is a response to warming of the South Atlantic sea surface temperature (SST) relative to the North Atlantic. Folland et al. (1986) formally demonstrated that persistently dry or wet periods over the Sahel region were accompanied by an inter-hemispheric contrast in SST; drought (pluvial) periods are linked to warm (cold) SSTs in the Southern Hemisphere (SH) relative to those in the Northern Hemisphere (NH). The pattern of contrasting SSTs coincided well with the dry trend in the 1970s and 1980s.

These studies used various approaches to interpret the long-term or short-term variability of the precipitation in Sahel. However, most studies focused only on the rainy season in Sahel and were limited to the relationship between precipitation variability during the rainy season and the SST surrounding Africa, or atmospheric circulation only around Africa. It would be useful to verify the relationship between variability of precipitation and inter-hemispheric SST contrast, including both the former decrease and the recent recovery of the rainfall in Sahel. The present study demonstrated the changing trends in inter-hemispheric global climate and concurrent inter-hemispheric SST that are involved with the recent increasing trend of precipitation in Sahel.

2. Data and Methods

The precipitation data used in this study are supplied from the Global Precipitation Climatology Centre (GPCC; ftp://ftp-anon.dwd.de/pub/data/gpcc/), and include a global analysis of monthly precipitation on earth’s land surface based on in situ rain-gauge data. We used the Full Data Reanalysis Product, which is based on all stations, near-real-time and non-real-time. The data cover the period from 1901 to 2007, and the spatial resolution is a global grid of 0.5° of latitude and 0.5° of longitude (Schneider et al., 2008). In the present study we analyzed the data from 1959 through 2007, which include the periods of the severe drought in Sahel and its recovery (1981-1985).

We also used National Centers for Environmental Prediction/National Center for Atmospheric Research (NCEP/NCAR) Reanalysis data sets (Kalnay et al., 1996); i.e. geopotential height, horizontal and vertical winds, and humidity data at the each levels. The SST data we used are from the recently available International Comprehensive Ocean-Atmosphere Data Set (ICOADS), which uses improved statistical methods that allow stable reconstruction using sparse data (Xue et al., 2003, Smith et al., 2008). The spatial resolution of this SST data is a global grid of 2.0° of latitude and 2.0° of longitude. We analyzed NCEP/NCAR Reanalysis data and ICOADS data over the same period, 1959 through 2007.

The definition of the Sahel region for this study is that part of the region in which climatological annual mean precipitation from 1959 through 2007 is from 100 to 500 mm/yr within the area to the west of 20°E (Figure 1). The long-term variation of the area-averaged annual mean precipitation within the Sahel region is shown in the upper panel of Figure 2. The minimum occurred in 1984, and the declining trend in precipitation before 1984 and the increasing trend after 1984 are readily apparent. We thus regard the year 1984 as the turning point in the precipitation trend. Hereafter, we divide our period of analysis into two sub-periods, before and after 1984. A linear regression lines showing the trend in each sub-period are also superimposed in Figure 2. This precipitation change in the Sahel region that is defined in this study is almost identical to those defined by other studies (e.g. Giannini et al., 2003, Thiaw and Mo, 2005, Hoerling et al., 2006, Nicholson and Wbster, 2007, Folts and McPhaden, 2008). The correlation coefficients of the Sahel precipitation by our definition with those by other studies are higher than 0.94. Therefore, the results and conclusions to be shown in this study do not depend on the choice of the definition of the Sahel region. We used these inter-annual time series and the trends in each sub-period to demonstrate the remote relationship between precipitation in other regions of the earth, inter-hemispheric atmospheric fields, and SSTs, and the long-term variation of the Sahel precipitation. All atmospheric fields, SSTs, and precipitation data analyzed in this study are annual mean values. We particularly emphasize the differences in the trends in the atmospheric and oceanic fields before and after 1984 to make the contrast clear.

3. Global structure of precipitation trend shifts

First, we demonstrate a global-scale horizontal distribution of the differences in precipitation trends between the years before and after 1984 (land areas in Figure 3). In addition to the reversal of the precipitation trend within Sahel, there were trend shifts over various areas of the earth. For example the northern part of Eurasia experienced the same trend shift as in Sahel; i.e., before 1984 this area experienced a decreasing trend in precipitation, whereas after 1984 it was an increasing trend. In contrast, the central region of South America and Australia show the opposite shift in trends. The overall shifts in the north Eurasia and Sahel are in phase, whereas the shifts in the Southern America overall are out of phase with Sahel.

4. Global structure of the trend shift in SST and atmospheric fields

Next we demonstrate the shift of the global SST trend (sea areas in Figure 3). A north-south inter-hemispheric anti-symmetric pattern is obvious. In the NH overall, SST experienced a warming trend after 1984 compared with before 1984, whereas there was a cooling trend in the SH after 1984 compared with before 1984.

On the basis of these results, we defined a north-south SST polarity index (NS-SST index) that is the difference between the area-weighted average SSTs in the NH and SH (NH minus SH). We compared the time series of the NS-SST index to the precipitation in Sahel (upper panel of Figure 2). The time series of the NS-SST index showed a minimum value in 1984 with a decreasing trend before 1984 and an increasing trend after 1984; a pattern remarkably similar to the precipitation variability in Sahel.

The NS-SST index only in the summer is also compared with the Sahel precipitation, because the rainy season in Sahel is in the Northern Hemisphere summer. Figure 4 shows the time series of the summer NS-SST index from May to October and the winter NS-SST index from November to April. These two time series are almost identical to each other, and remarkable similar to that of the annual mean NS-SST index (upper panel of Figure 2), indicating that the seasonality of the inter-hemispheric SST contrast is small. The correlation coefficients of the annual mean NS-SST index with the summer NS-SST and the winter NS-SST are 0.97 and 0.96, respectively. The correlation coefficients of the Sahel precipitation with the annual mean NS-SST, summer NS-SST and winter NS-SST are 0.52, 0.57 and 0.61, respectively.

We also examined the north-south polarity of precipitable water (NS-PW index) and the atmospheric thickness between 300 hPa and 1000 hPa (NS-thickness index) (bottom panel of Figure 2), after calculating these indices in the same manner as the NS-SST index. The time series of the NS-PW and NS-thickness indices are also remarkably similar to the precipitation variability in Sahel and the NS-SST index.

We also examined the lag-correlation between the precipitation in Sahel and the NS-SST, NS-PW and NS-thickness indices. The maximum correlations occur when the individual indices precede the Sahel precipitation by two years. The 2-year-lag correlation coefficients of the Sahel precipitation with the NS-SST, NS-PW and NS-thickness indices are 0.58, 0.54 and 0.47, respectively. The correlation of the Sahel precipitation with the NS-SST index is higher than that with the indices of north-south inter-hemispheric SST polarity in individual large oceans; the correlation coefficients between the Sahel precipitation and the north-south polarity of SST in the Atlantic, Indian and Pacific Oceans are 0.54, 0.49 and 0.44, respectively. These properties suggest that the global NS-SST polarity remotely influences the north-south polarity of atmospheric temperature and humidity, and additionally the precipitation in Sahel.

5. North-south SST polarity and its associated global patterns

In this section we show horizontal structures of SST and land precipitation correlated with the NS-SST index. The contrasting positive and negative correlations in the NH and SH, respectively, are evident in all large oceans (sea areas in upper panel of Figure 5). Overall, large signatures can be seen in large oceans covering mid and high latitudes in both hemispheres, but not in tropical regions.

Land areas show a similar contrast in precipitation, with significant positive correlations over Sahel and northern Eurasia, and significant negative correlations over South America and central Australia (land areas in upper panel of Figure 5). This NS contrast is also similar to the trend shifts in global precipitation, and they accord well with the trend shifts of the NS-SST index and the precipitation. Horizontal structures of SST and land precipitation correlated with the NS-SST index only during the northern hemisphere summer is also demonstrated (bottom panel of Figure 5). Similarly, the contrasting positive and negative correlations in the NH and SH, respectively, are evident in all large oceans and land areas.

Next, we show the correlations between the NS-SST index and atmospheric fields. We calculated the correlation coefficients between the NS-SST index and the velocity potential at 0.2101 (upper troposphere) and 0.995 (lower troposphere) sigma levels to diagnose the relationships of the divergent fields (Figure 6). The correlation was positive for the upper troposphere above northern Africa, and in contrast, the correlation was negative for the regions above the Atlantic and South America (upper panel of Figure 6). In contrast, the lower troposphere around all of Africa showed a negative correlation, whereas over South America and the Southern Ocean there were positive correlations (bottom panel of Figure 6). These patterns suggest that recently northern Africa experiences strengthening of the convergence at the lower troposphere and the divergence at the upper troposphere in association with the warmer SST in the NH than in the SH, whereas the Atlantic and South American regions show the reverse.

These horizontal patterns are mainly associated with long-term variation of the inter-hemispheric contrast in SST, because correlated horizontal patterns of the velocity potential with a filtered short-term time series of the NS-SST index are unclear (Figure not shown). The correlation between the NS-SST index and the streamfunction also shows that northern Africa and the northern tropical Atlantic at the upper troposphere experience a strengthening of the cyclonic rotation in association with the warmer SST in the NH than in the SH, and southern Africa experiences the reverse (upper panel of Figure 7). At the same time, the lower troposphere above northern Africa experiences a strengthening of the anticyclonic rotation, whereas above South Africa and the southern tropical Atlantic the inverse occurs (bottom panel of Figure 7). These horizontal patterns are mainly associated with long-term variation of the inter-hemispheric contrast in SST, because correlated horizontal patterns of the streamfunction with a filtered short-term time series of the NS-SST index are unclear (Figure not shown).

We calculated the correlation coefficients for the specific humidity and the meridional and vertical winds with the NS-SST index (Figure 8). Sahel experiences ascending winds and wet conditions with inter-hemispheric northward flow in the lower troposphere when the NS-SST index is positive, contrasting with descending winds and dry anomalies over southern Africa and South America. In particular, there is a notable contrast in specific humidity; Sahel is wet, while the South Atlantic and Indian Oceans are dry in association with SH SSTs lower than NH SSTs. These signatures are detected not only in the Sahel region but also over the rest of the world. We performed the same correlation analyses using north-south SST polarity indices only within the Atlantic Ocean. However, we found no clear differences or patterns such as those demonstrated above.

6. Discussion

We confirmed that there was a decreasing trend in Sahel precipitation before 1984 and an increasing trend after 1984. This trend shift agrees with previous studies (e.g. Fall et al., 2006, Hoerling et al., 2006, Hagos and Cook, 2008). Our results and their implications can be summarized as follows.

1) The reversal of the trend in precipitation occurred not only within Sahel but also over other regions of the earth. The trend shifts over the north Eurasia and Sahel were in phase overall, whereas those over the South America were out of phase with Sahel. In the broadest terms, the trend shift over the NH was out of phase with that of the SH, except for North America. Therefore, there was a north-south polarity in the precipitation trends.

2) The trend shift of Sahel precipitation was remarkably similar to the trend shift of the SST contrast between NH and SH. A trend of warming NH SST relative to SH SST occurred concurrently with the increasing trend of NH precipitation and increasing precipitation over Sahel. Our NS-SST index successfully captured the recent increasing trend of the Sahel precipitation, confirming a previous finding by Folland et al. (1986) that the cooling of NH SST relative to the SH SST accounted for the decreasing trend in Sahel precipitation that occurred in 1960-1970.

3) Both the wintertime and summertime SST contrasts between NH and SH are related to the interannual Sahel rainfall, suggesting that very far oceans from Africa

influence the Sahel rainfall beyond a season.

4) The NS-SST polarity index, which includes all of the world's oceans, accounted for the precipitation variability in Sahel better than the North-South SST polarity index of any individual ocean. Although the local Atlantic SST influences the Sahel precipitation, as pointed out by Herling et al. (2006) and Hagos and Cook (2008), our results suggest the influence of remote inter-hemispheric NS-SST contrast.

5) The trend shift of the NS-SST contrast is also associated with trend shifts of inter-hemispheric atmospheric contrasts. Concurrent with the warming trend of NH SST relative to SH SST was a warming trend of the tropospheric air temperature and an increasing trend of the specific humidity in the NH relative to that in the SH. There was also a trend of a strengthening updraft over Sahel in association with the strengthening trend of meridional circulation from SH to NH in the lower troposphere, and from NH to SH in the middle troposphere.

These results suggest that the NS-SST contrast determines the worldwide precipitation trends through changes of atmospheric inter-hemispheric circulations. Warmer NH SST relative to SH SST possibly influences the warm and humid conditions of the NH atmosphere relative to the SH atmosphere. This atmospheric north-south contrast possibly strengthens an inter-hemispheric meridional circulation, and stimulates (depresses) the precipitation in the NH (SH). Because the NCEP/NCAR reanalysis data for humidity and vertical motion from the pre-satellite era are not as accurate as those from recent years, this mechanism is suggested as a possible candidate for explaining the present results. However, additional explanations are required for why the signature of the precipitation trend shift over the Sahel is particularly large. In addition, further studies are required on the causes of long-term variation of the north-south SST polarity.

Acknowledgements

We thank K. Fukuyama and Y. Sekine for their valuable suggestions and comments. Comments of anonymous reviewers are also very helpful. Furthermore, we express our appreciation to the GPCC for the precipitation data and to NOAA/OAR/ESRL PSD for the global SST data.

References

Fall S., Semazzi FHM, Niyogi DDS, Anyah RO, Bowden J. 2006. The spatiotemporal climate variability over Senegal and its relationship to global climate. *International Journal of Climatology* **26**: 2057-2076.

Folland CK., Palmer TN, Parker DE. 1986. Sahel rainfall and worldwide sea temperatures, 1901-85. *Nature* **302**: 602-607, DOI:10.1038/320602a0.

Folts GR, McPhaden MJ. 2008. Trends in Saharan dust and tropical Atlantic climate during 1980-2006. *Geophysical Research. Letters* **35**: DOI:10.1029/2008GL035042.

Giannini A, Sravanan R, Chang P. 2003. Oceanic Forcing of Sahel Rainfall on Interdecadal Time Scales. *Science* **302**: 1027-1030.

Hagos SM, Cook KH. 2008. Ocean Warming and Late-Twentieth-Century Sahel Drought and Recovery. *Journal of Climate* **21**: 3797-3814.

Hoerling M, Hurrell J, Eischeid J, Phillips A. 2006. Detection and Attribution of

Twentieth-Century Northern and Southern African Rainfall Change. *Journal of Climate* **19**: 3989-4008.

Kalnay E, Kanamitsu M, co-authors. 1996. The NCEP/NCAR 40-year Reanalysis Project. *Bulletin of the American Meteorological Society* **77**: 437-471.

Nicholson ES, Webster PJ. 2007. A physical basis for the interannual variability of rainfall in the Sahel. *Quarterly Journal of the Royal Meteorological Society*: DOI:10.1002/qj.104.

Omotosho BJ. 2008. Pre-rainy season moisture build-up and storm precipitation delivery in the West African Sahel. *International Journal of Climatology* **28**: 937-946, DOI:10.1002/joc.1548.

Schneider U, Fuchs T, Christoffer AM, Rundolf B. 2008. Global Precipitation Analysis Product of the GPCC. Deutscher Wetterdienst, Offenbach a. M., Germany, 1-12.

Smith TM, Reynolds RW, Peterson TC, Lawrimore J. 2008. Improvements to NOAA's Historical Merged Land-Ocean Surface Temperature Analysis (1880-2006). *Journal of Climate* **21**: 2283-2296.

Thiaw WM, Mo KC. 2005. Impact of Sea Surface Temperature and Soil Moisture on Seasonal Rainfall Prediction over the Sahel. *Journal of Climate* **18**: 5330-5343.

Xue Y, Smith TM, Reynolds RW. 2003. Interdecadal changes of 30-yr SST normals during 1871-2000. *Journal of Climate* **16**: 1601-1612.

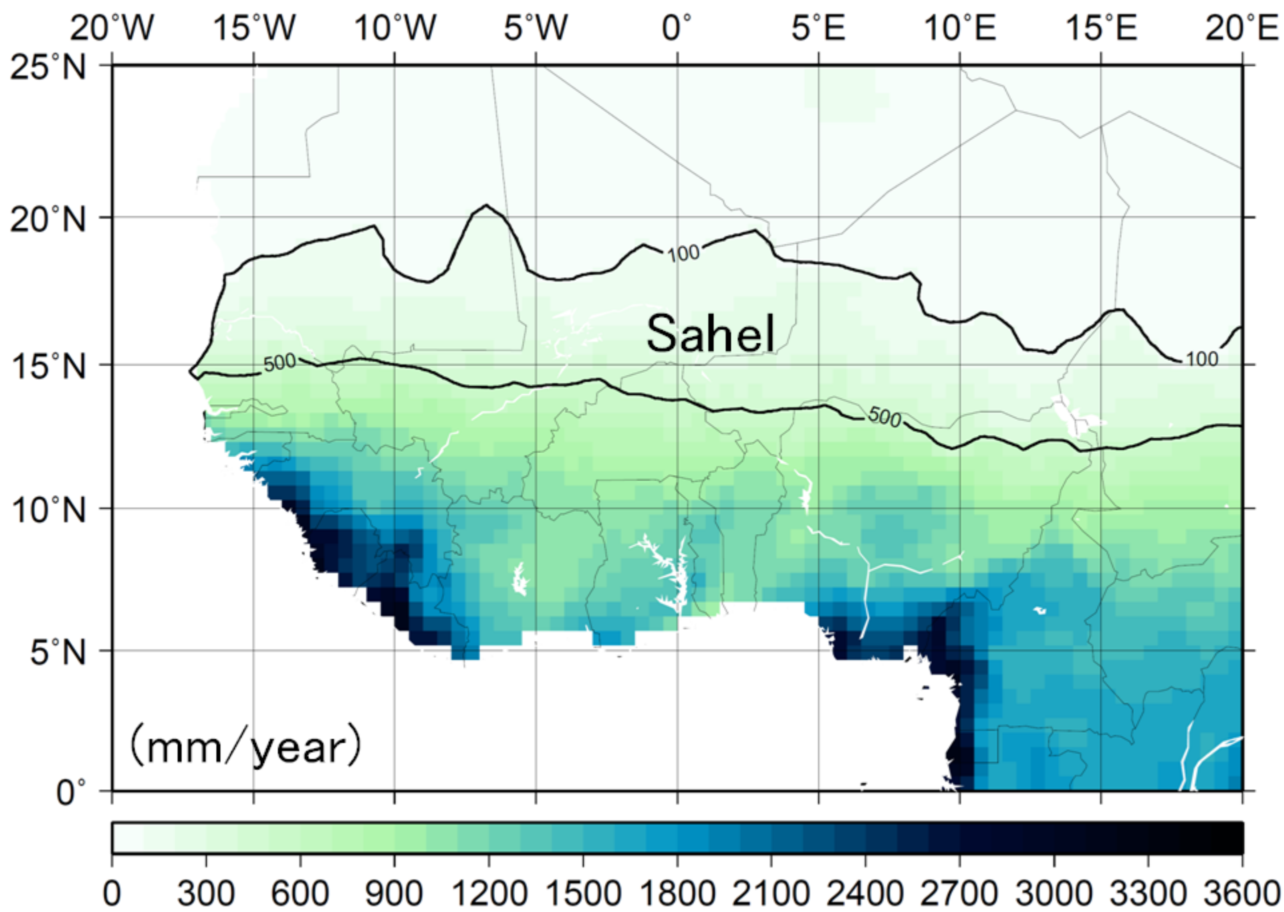

Figure 1. Climatological annual precipitation (mm/yr) in northwestern Africa and the Sahel region defined in this study (100 - 500 mm/yr). Thick lines indicate isohyets at the 100 and 500 mm/yr.

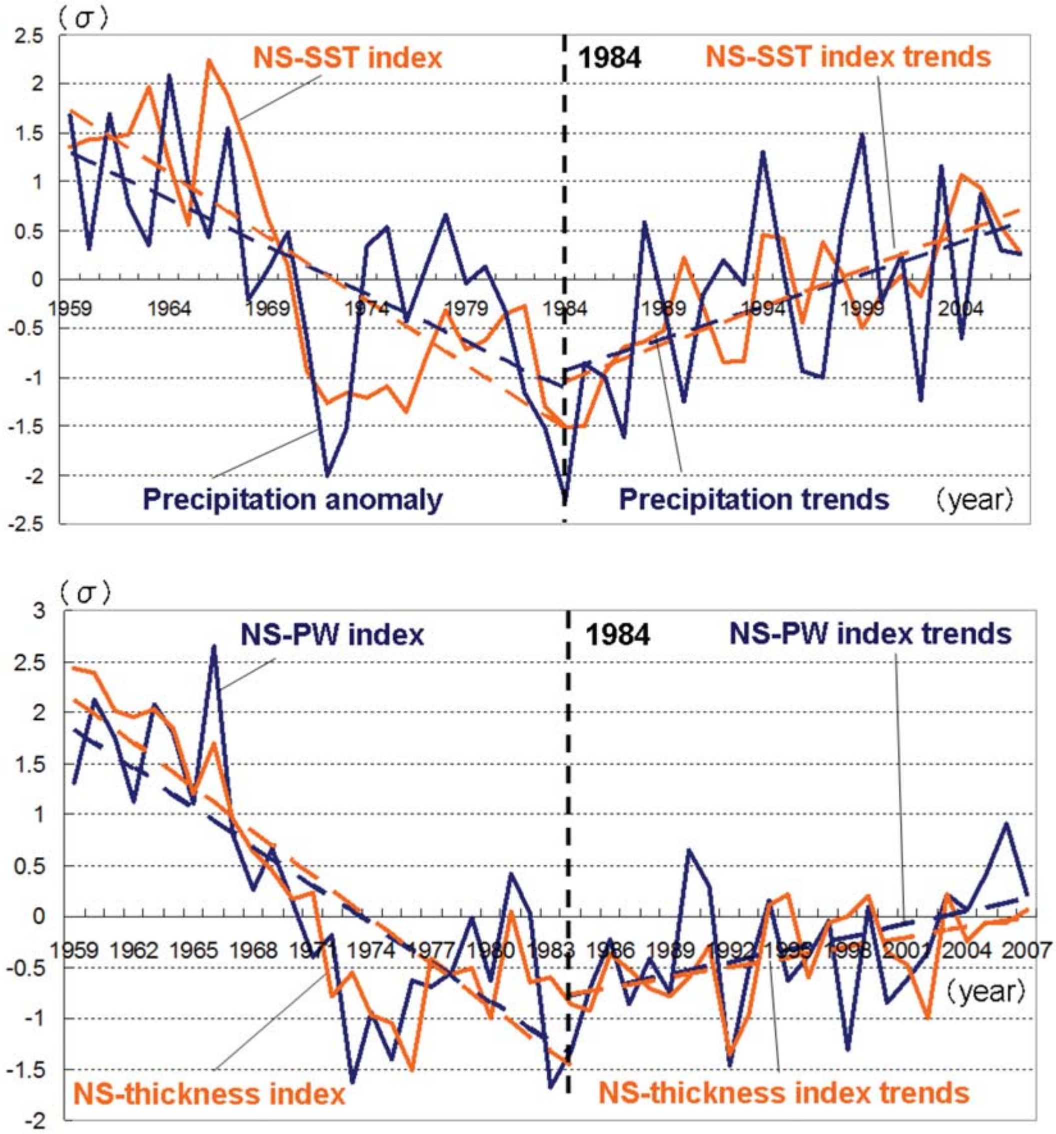

Figure 2. (Top) Normalized precipitation anomalies (dark blue) in Sahel and the north-south SST (NS-SST) polarity index (orange; the difference between NH and SH area-averaged SSTs [NH - SH]), and their respective linear regression lines before and after 1984. (Bottom) Normalized time series of the north-south precipitable water polarity index (NS-PW index; dark blue lines) and the north-south thickness polarity index (NS-thickness index; orange lines), and their linear regression lines before and after 1984. These indices are the difference between the area-averaged values over the Northern and Southern Hemispheres (NH minus SH).

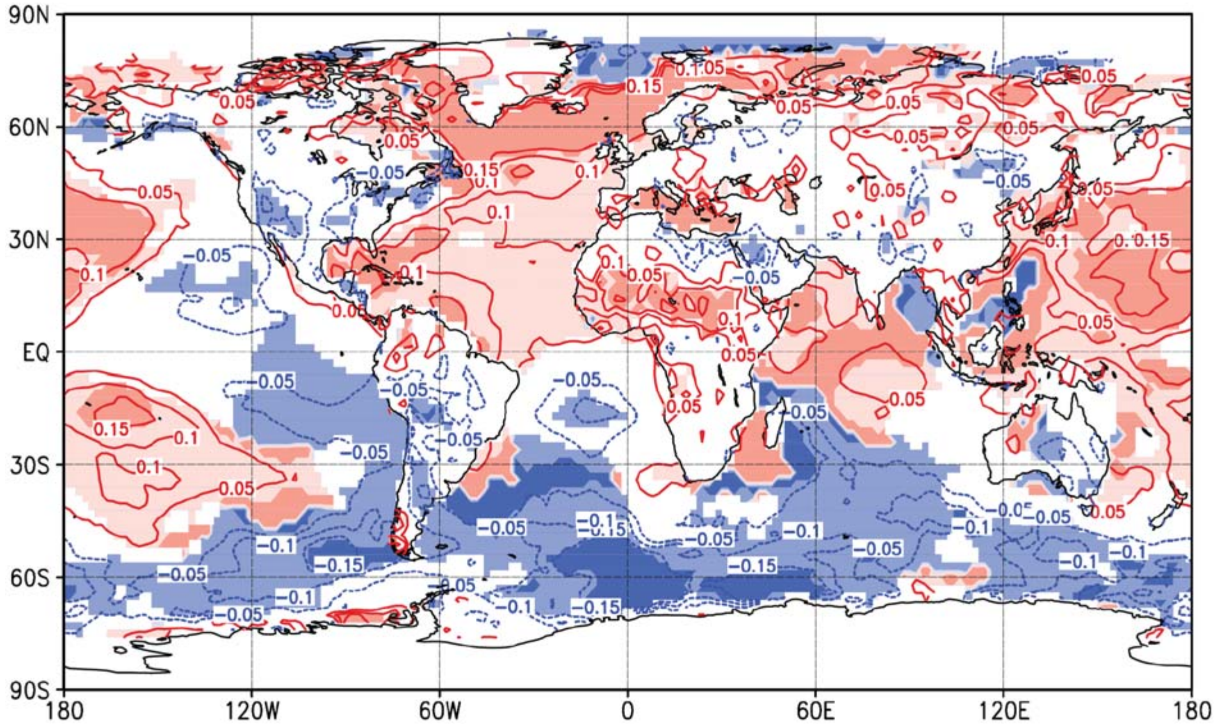

Figure 3. Trend anomalies, here defined as the differences between normalized SST (sea areas) and precipitation (land areas) trends after 1984 and before 1984 ([post-1984] minus [pre-1984]). Red (blue) contours indicate positive (negative) trend anomalies and contour intervals are 0.05/yr. Dark reddish and bluish shaded areas are significant at the 10% level based on a Student's t-test for the trends both before and after 1984. Light shaded areas are significant at the 10% level based on a Student's t-test for the trends either before or after 1984.

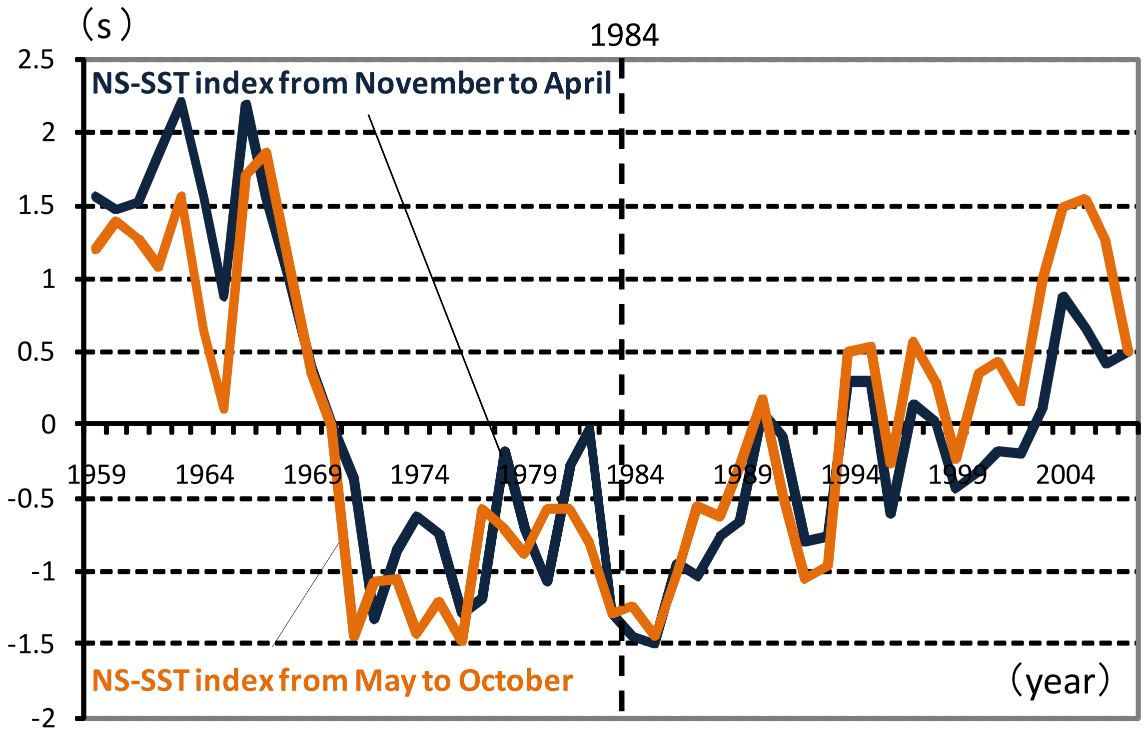

Figure 4. Normalized NS-SST polarity indices of northern hemisphere summer and winter (orange; the difference between NH and SH from May through October, dark blue; the difference between NH and SH from November through April). These indices are the difference between the area-averaged values over the Northern and Southern Hemispheres (NH minus SH).

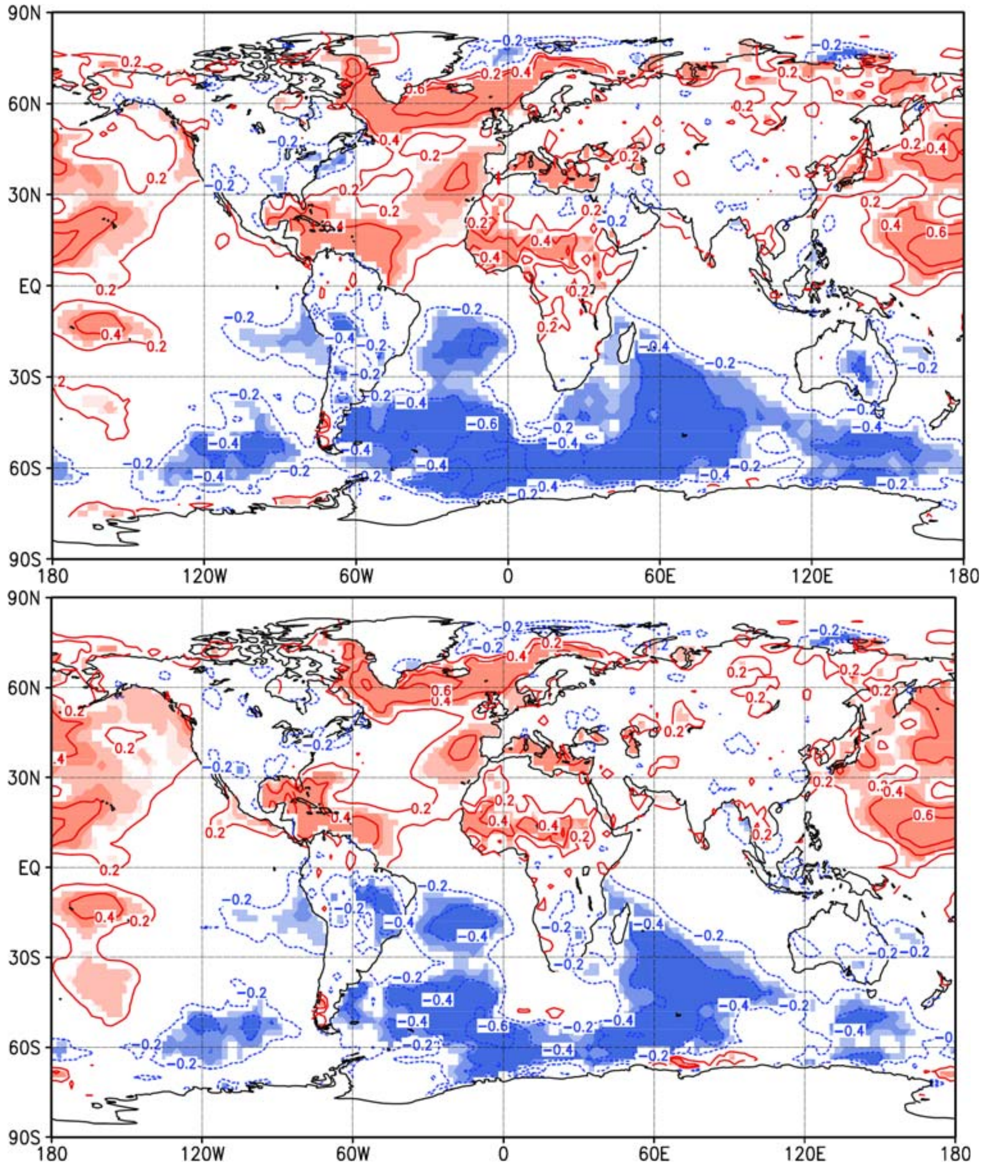

Figure 5. (Top) Correlation coefficients between the annual mean NS-SST index averaged from January through December, and the annual mean global SST (ocean areas) or precipitation (land areas) anomalies. (Bottom) Correlation coefficients between the summer NS-SST index averaged from May through October, and the annual mean global SST (ocean areas) or precipitation (land areas) anomalies. Reddish (bluish) color indicates positive (negative) correlations and contour intervals are 0.2. Shaded areas are significant at the 1%, 5% or 10% levels (dark to light) based on a Student's t-test.

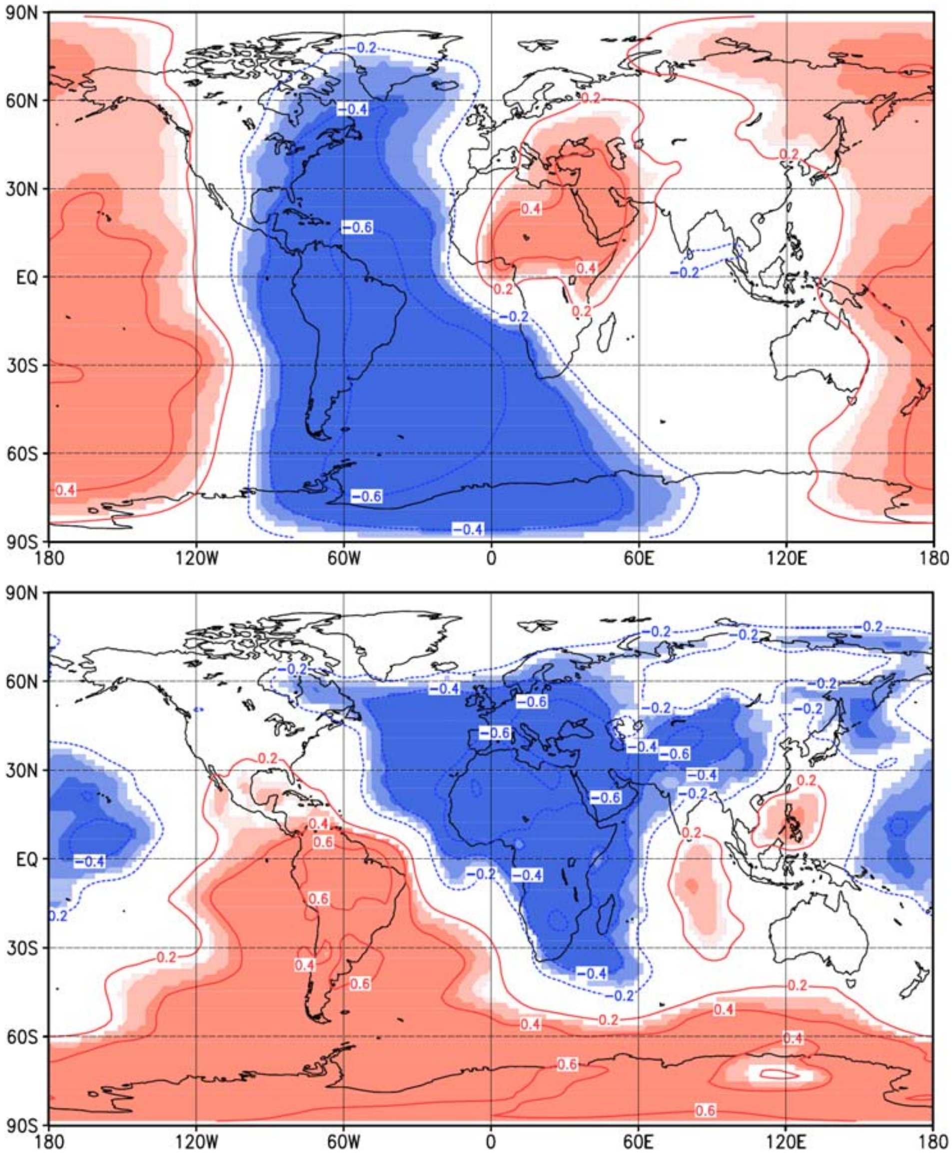

Figure 6. As in upper panel of Figure 5 except for between the NS-SST index and velocity potential at 0.2101 sigma level (top) and at 0.995 sigma level (bottom).

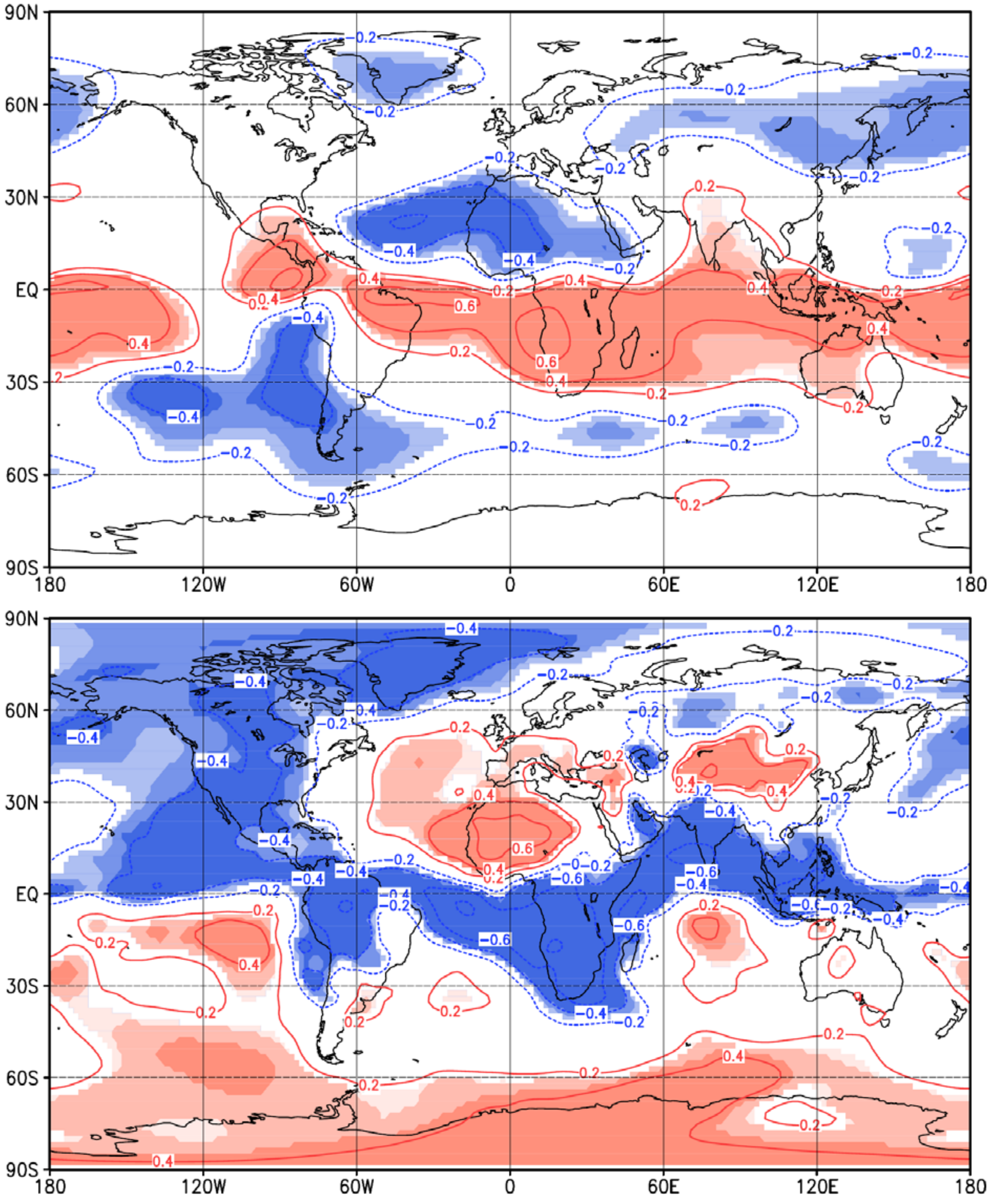

Figure 7. As in upper panel of Figure 5 except for between the NS-SST index and streamfunction at 0.2101 sigma level (top) and at 0.995 sigma level (bottom).

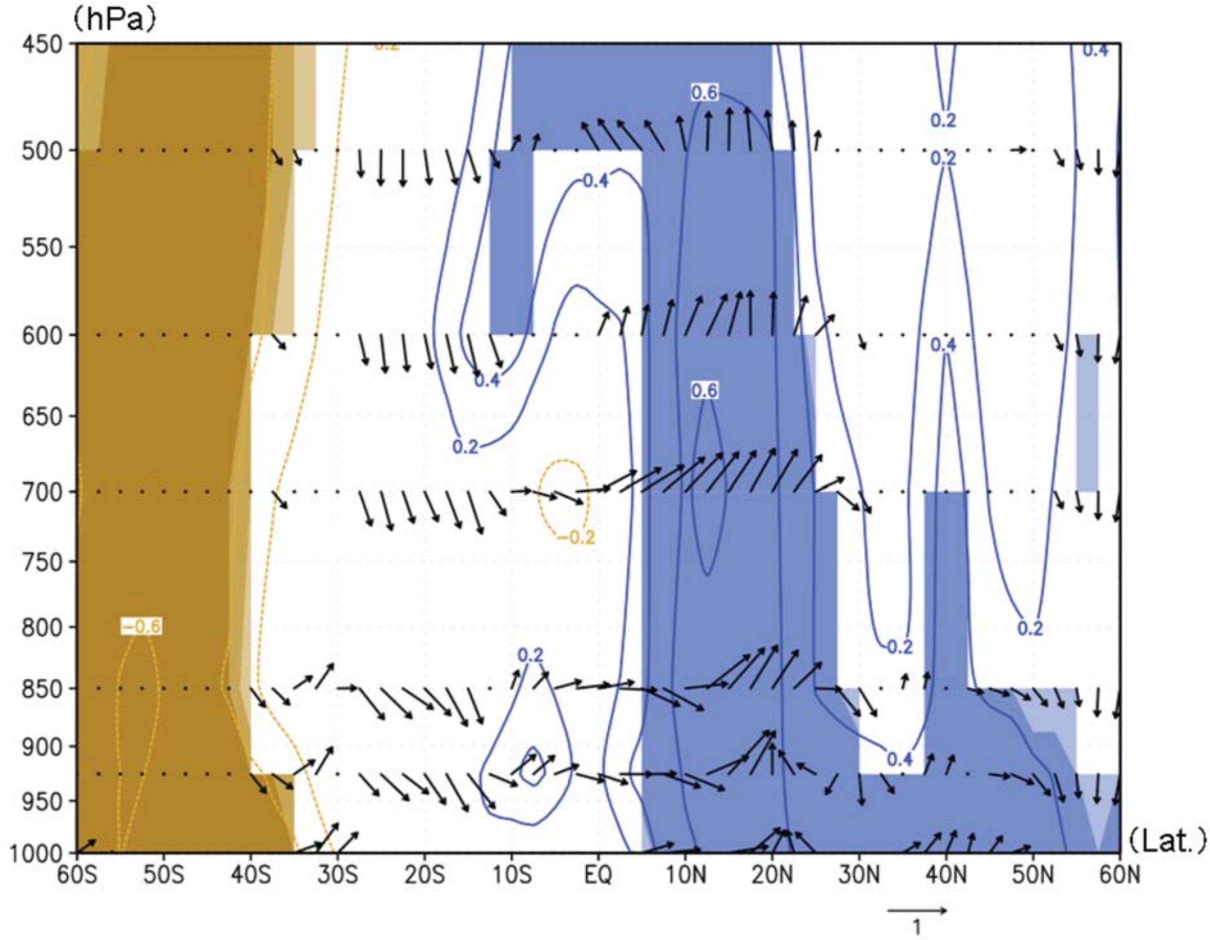

Figure 8. Vertical cross-section of the coefficients of correlation of the NS-SST index with the specific humidity (shaded areas and contours), and with the meridional and vertical winds averaged from 20°W through 50°E (arrows). The vectors indicated by arrows show the correlation coefficients of meridional and vertical components with the NS-SST index. Vectors upward and northward indicate positive correlations. Bluish (brownish) color indicates positive (negative) correlations with specific humidity. Contour intervals are 0.2. Shaded areas are the same as in Figure 5. The vectors included here are those where the level of significance exceeded 10% for either the meridional or vertical wind.